

RESEARCH ARTICLE | FEBRUARY 18 2026

# Surface termination of $\beta\text{-Ga}_2\text{O}_3(100)$ as-cleaved single crystals

Ming-Chao Kao ; Lukas Paul Schewe ; Arub Akhtar ; Alina Vlad ; Thomas F. Keller ; Karsten Henkel ; Saud Bin Anooz ; Andreas Popp ; Zbigniew Galazka ; Jan Ingo Flege ; Andreas Stierle ; Vedran Vonk  



*Appl. Phys. Lett.* 128, 071601 (2026)

<https://doi.org/10.1063/5.0309937>



## Articles You May Be Interested In

Two-scale structure of the current layer controlled by meandering motion during steady-state collisionless driven reconnection

*Phys. Plasmas* (July 2004)

Single particle motion near an X point and separatrix

*Phys. Plasmas* (June 2004)

18 February 2026 15:04:15

## AIP Advances

### Why Publish With Us?



**21DAYS**  
average time  
to 1st decision



**OVER 4 MILLION**  
views in the last year



**INCLUSIVE**  
scope

[Learn More](#)



# Surface termination of $\beta$ -Ga<sub>2</sub>O<sub>3</sub>(100) as-cleaved single crystals

Cite as: Appl. Phys. Lett. **128**, 071601 (2026); doi: 10.1063/5.0309937

Submitted: 30 October 2025 · Accepted: 2 February 2026 ·

Published Online: 18 February 2026



View Online



Export Citation



CrossMark

Ming-Chao Kao,<sup>1,2</sup> Lukas Paul Schewe,<sup>3</sup> Arub Akhtar,<sup>4</sup> Alina Vlad,<sup>5</sup> Thomas F. Keller,<sup>1,2</sup> Karsten Henkel,<sup>3</sup> Saud Bin Anooz,<sup>4</sup> Andreas Popp,<sup>4</sup> Zbigniew Galazka,<sup>4</sup> Jan Ingo Flege,<sup>3</sup> Andreas Stierle,<sup>1,2</sup> and Vedran Vonk<sup>1,a)</sup>

## AFFILIATIONS

<sup>1</sup>Centre for X-ray and Nano Science CXNS, Deutsches Elektronen-Synchrotron DESY, Notkestraße 85, 22607 Hamburg, Germany

<sup>2</sup>Department of Physics, University of Hamburg, Jungiusstraße 11, 20355 Hamburg, Germany

<sup>3</sup>Applied Physics and Semiconductor Spectroscopy, Brandenburg University of Technology Cottbus-Senftenberg, D-03046 Cottbus, Germany

<sup>4</sup>Leibniz-Institut für Kristallzüchtung, Max-Born-Straße 2, D-12489 Berlin, Germany

<sup>5</sup>Synchrotron SOLEIL, L'Orme des Merisiers, 91190 Saint-Aubin, France

<sup>a)</sup> Author to whom correspondence should be addressed: [vedran.vonk@desy.de](mailto:vedran.vonk@desy.de)

## ABSTRACT

The surface of  $\beta$ -Ga<sub>2</sub>O<sub>3</sub> single crystals cleaved along their (100) plane is investigated using surface x-ray diffraction and atomic force microscopy. The results show the surface to consist of a single, so-called B-termination, which means that the crystal cleaves at planes formed by edge-sharing oxygen octahedra, thereby breaking the longest and weakest Ga–O bonds. Refinement of the atomic positions results in small displacements from the bulk structure, at most approximately 0.01 Å. Atomic force microscopy suggests that relatively large terraces form together with steps of half the a-axis length of approximately 0.6 nm, which means that terraces have the same atomic termination, related by the crystal symmetry. These results are important as a fundamental property of  $\beta$ -Ga<sub>2</sub>O<sub>3</sub> when processed or used in various semiconductor applications.

© 2026 Author(s). All article content, except where otherwise noted, is licensed under a Creative Commons Attribution (CC BY) license (<https://creativecommons.org/licenses/by/4.0/>). <https://doi.org/10.1063/5.0309937>

Beta-type gallium oxide ( $\beta$ -Ga<sub>2</sub>O<sub>3</sub>) is a transparent semiconductor with a wideband gap of about 4.85 eV,<sup>1,2</sup> making it highly promising for high-power electronics<sup>3–7</sup> and solar-blind UV photodetectors.<sup>8</sup> For high-power switching, Ga<sub>2</sub>O<sub>3</sub> is predicted to outperform SiC and GaN technologies due to a three times higher calculated critical field strength,<sup>3</sup> making it an attractive material for efficient next-generation power conversion systems with reduced energy loss. Processing of  $\beta$ -Ga<sub>2</sub>O<sub>3</sub> down to the nano-scale<sup>9–11</sup> is discussed for most of the possible applications. The atomic surface structure and related surface energy are of fundamental importance for mechanistic studies of (epitaxial) growth, shape, and processing of nano-scaled crystallites, and adsorption properties, as exploited in gas-sensing applications.<sup>12,13</sup> In this study, we focus on single crystals cleaved along the (100) plane, which can be used as substrates for high-power semiconductor devices. Previous experimental approaches have provided some insights into the possible termination of this surface,<sup>14–16</sup> but did not provide the full 3D crystallographic details, needed for a detailed comparison with

recent density functional theory (DFT) calculations.<sup>17–19</sup> As a result, a full and detailed description of the geometric structure is still outstanding. In addition, the study of a cleaved surface provides information about the details of such planes, which is relevant for fracture formation and relatively easy substrate preparation of this technologically interesting oxide material. In this work, we use synchrotron-based Surface X-ray Diffraction (SXRD) and Atomic Force Microscopy (AFM) to determine, with high resolution, the atomic structure and surface termination of this technologically relevant surface.

High-quality  $\beta$ -Ga<sub>2</sub>O<sub>3</sub> single crystals were grown using the Czochralski method at the Leibniz-Institut für Kristallzüchtung (IKZ).<sup>20,21</sup>  $\beta$ -Ga<sub>2</sub>O<sub>3</sub> has a monoclinic crystal structure with the space group C2/m. The conventional unit cell contains four formula units, with gallium atoms (green) occupying both tetrahedral and octahedral coordination sites as shown in Fig. 1. The lattice parameters are  $a = 12.214$  Å,  $b = 3.037$  Å,  $c = 5.798$  Å,  $\alpha = 90^\circ$ ,  $\beta = 103.83^\circ$ , and  $\gamma = 90^\circ$ .<sup>22–24</sup> All fractional coordinates listed in Table S3 and used for

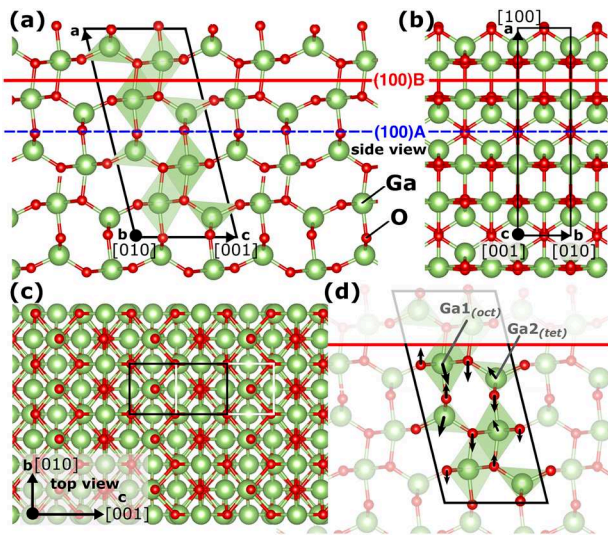


**FIG. 1.** Two possible surface terminations of  $\beta$ - $\text{Ga}_2\text{O}_3$  (100) are indicated by red and blue dashed lines. The A-termination is a plane through the corner-sharing oxygen octahedra and tetrahedra. The B-termination is a plane through edge-sharing oxygen octahedra. The average broken bond length for the B-termination is slightly higher than for the A-termination. The unit cell is shown in the (a) [100]/[001], (b) [100]/[010], and (c) [010]/[001] planes. (d) The fitted displacements of gallium atoms at the octahedral ( $\text{Ga}_{1(\text{oct})}$ ) and tetrahedral ( $\text{Ga}_{2(\text{tet})}$ ) sites, as well as the oxygen atoms, for the B-terminated surface are shown. The length of the displacement arrows is proportional to the magnitude of the displacement, but it is scaled up by a factor of approximately 100 to enhance visibility.

Crystal Truncation Rod (CTR) fitting are defined with respect to this unit cell.

The single crystals were cleaved along the (100) plane under ambient conditions,<sup>20,21</sup> and their surfaces were used for all subsequent measurements without further polishing or chemical etching. The samples were prepared with dimensions of  $10 \times 10 \text{ mm}^2$  and a thickness of around 0.1 mm. Prior to use, all surfaces were cleaned in an ultrasonic bath with ethanol and isopropanol for 30 min.

Atomic force microscopy (AFM) was performed in air using tapping mode with a silicon cantilever at the DESY NanoLab.<sup>25</sup> The nominal tip radius was 8 nm, the resonance frequency was 301.6 kHz, and the scan rate was 0.5 kHz. The data were analyzed using Gwyddion software,<sup>26</sup> as described in detail in Fig. S1 and Table S1.

Crystal Truncation Rod (CTR) data were collected at the *Surfaces and Interfaces X-ray Scattering* (SIXS) beamline of the French synchrotron facility SOLEIL, using a photon energy of 18.42 keV. The measurements were performed in grazing incidence geometry using a diffractometer hosting a UHV chamber, which enables *in situ* experiments with sample heating up to 1000 °C and controlled oxygen dosing. Scattered intensities were recorded using a two-dimensional hybrid photon-counting detector XPAD S140.<sup>27</sup> Both the preparation and measurement chambers maintained background pressures in the low  $10^{-10}$  mbar range. Structure factors (SFs) were obtained by integrating the measured data with the BINoculars package.<sup>28</sup> Subsequent surface structure refinement was conducted using the ROD program from the ANAROD package.<sup>29</sup>

Surface x-ray diffraction (SXRD) is a powerful technique for determining the atomic structure of crystal surfaces with sub-angstrom

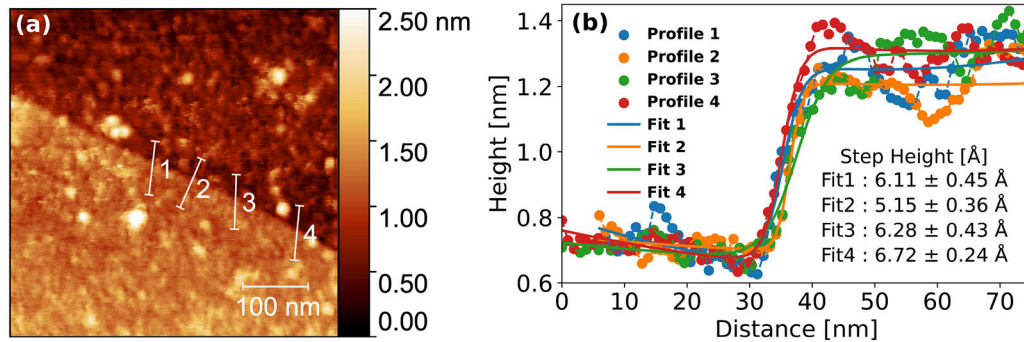
precision. The abrupt ending of a crystal's periodic atomic arrangement at its surface results in additional diffracted intensity between the Bragg peaks in the surface normal direction, known as Crystal Truncation Rods (CTRs).<sup>30</sup> The intensity along these rods is calculated by evaluating the structure factor, which contains information about the atomic positions, site occupancies, and Debye-Waller factors.<sup>29</sup> In general, the best CTR data quality is obtained for very smooth surfaces since its intensity is affected by surface roughness.<sup>31</sup>

Pre-characterization of the as-cleaved bulk crystal was performed using low-energy electron diffraction (LEED) at the SIXS beamline. The sample was annealed at 400 °C in an oxygen partial pressure of  $10^{-6}$  mbar for 1 h to effectively remove contaminants. After cleaning, the crystal was characterized by LEED over a range of electron energies to verify its structure and overall crystal quality. Then, the sample was transferred in vacuum to the main diffraction chamber for the SXRD measurements.

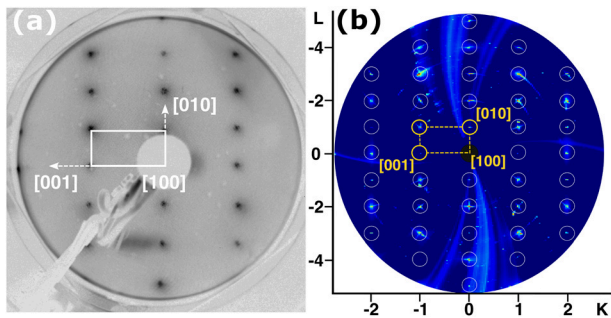
The surface morphology of the cleaned, as-cleaved  $\beta$ - $\text{Ga}_2\text{O}_3$ (100) surface was investigated using AFM, and Fig. 2(a) presents a typical image. The most obvious feature is a step that separates two terraces. Detailed analysis by fitting a Boltzmann bent step function across the step at several positions [see Fig. 2(b)] reveals a step height of approximately 0.6 nm, which represents half the unit cell along the a-axis. Such step heights have also been reported previously.<sup>15,32</sup> The average step density on such a cleaved surface is expected to be very low, and scanning the surface at a random position has a low probability of capturing a step. This is similar to the structurally related oxide crystal muscovite mica, which also exhibits a monoclinic structure and contains an easy cleave plane, resulting in millimeter-sized terraces.<sup>33</sup> Apart from such steps, the AFM images show the presence of many particle-like features. The nature and origin of these features are at present still unclear, but similar structures are also visible in high-quality substrates prepared by polishing and annealing for epitaxial growth.<sup>32,34</sup> Such epi-ready substrates with well-defined miscuts show a clear step-and-terrace structure whereby these particle-like features seem to accumulate at the steps, in contrast to the as-cleaved surface studied here, where they appear randomly over the entire surface. Nevertheless, the analysis of the AFM images shows that the as-cleaved surfaces exhibit a flat and smooth terrace structure, which is a prerequisite for SXRD experiments as described hereafter.

Figure 3(a) shows the LEED image of the as-cleaved (100) surface. A clear pattern of spots that reveals the rectangular surface cell is observed, indicating a well-ordered crystalline structure. Similarly, an in-plane reciprocal space map, recorded with SXRD [see Fig. 3(b)], also shows a well-defined crystal structure. The SXRD data also clearly show mosaicity, which indicates that rotated grains exist. Nevertheless, within the arcs of intensity, there is one clear most intense component, which indicates the presence of one large single-crystal-like block.

The obtained experimental CTRs (see Fig. 4) are compared with the various possible surface terminations, as further detailed in Figs. S2–S4. A first comparison, by evaluating the  $\chi^2$  values listed in Table S2, based on CTR simulations assuming a bulk termination, i.e., no further atomic relaxations and only optimizing the overall scale factor, clearly favors the (100)B surface, with a significantly smaller difference between the other terminations. A density functional theory study<sup>17</sup> ranked the (100)B surface to have the lowest and the (100)A the second lowest surface energy, which leads us to compare these two terminations in more detail. The A-termination consists of singly bound O



**FIG. 2.** (a) AFM image of the as-cleaved  $\beta$ - $\text{Ga}_2\text{O}_3(100)$  single crystal, showing the surface morphology and step structure. Four representative line profiles are indicated on the image. (b) Height profiles corresponding to the four indicated lines in (a), together with their fits. The profiles reveal a step height of approximately half the unit cell.



**FIG. 3.** LEED patterns and in-plane reciprocal space maps of the  $\beta$ - $\text{Ga}_2\text{O}_3(100)$  single crystal after annealing. (a) LEED pattern recorded at an electron energy of 98.4 eV. (b) Two-dimensional in-plane reciprocal space map, acquired at an x-ray energy of 18.42 keV. Both figures are indexed by (K, L).

atoms resulting in a mainly oxygen-terminated surface, which cuts through a plane of corner-sharing oxygen octahedra and tetrahedra. The (100)B termination consists of O atoms bound to two Ga atoms and corresponds to a plane cutting through edge-sharing oxygen octahedra. The average broken bond lengths for terminations (100)A and (100)B are 1.94 and 2.00 Å, respectively.<sup>23</sup> The (100) surface can be classified as a Tasker II-type surface<sup>35</sup> where the details of the surface structure lead to the (100)A being polar and (100)B non-polar.<sup>36</sup>

Refinement against the CTR data of the atomic positions in the topmost layers leads to by far the best fit for the B termination ( $\chi^2 = 1.2$ ) than for A ( $\chi^2 = 12.1$ ). Actually, the fit using the A termination does not converge within the maximum displacement limits of approximately 1 Å, as set in the software. The atomic positions of the Ga atoms were fitted along the [100] and [001] directions, thereby following the underlying monoclinic symmetry as present in the bulk crystal. For the oxygen atoms, which have a much lower scattering power, it was found that only refinement along the out-of-plane direction was stable, and therefore the in-plane positions were kept fixed at their bulk values. The maximum displacement from the bulk position in the case of termination B is about 0.1 Å, which shows that it is a nearly bulk-terminated surface. The best CTR fit result for termination B is shown in Fig. 4. Schematically, the atomic displacements from their bulk positions are shown in Fig. 1, and the final fractional coordinates as well as the Debye–Waller factors are listed in Table S3.

The refined atomic positions agree very well with the density functional theory study by Mu *et al.*<sup>17</sup> In particular, the CTR analysis shows that the topmost octahedrally coordinated Ga atom ( $\text{Ga}_{1\text{oct}}$ ) relaxes inward by approximately 0.1 Å and the topmost tetrahedrally coordinated atom ( $\text{Ga}_{2\text{tet}}$ ) outward by approximately 0.04 Å, resulting in a less buckled Ga plane. Similar relaxations were also found by another DFT study by Bermudez;<sup>19</sup> however, in that study, these were found to extend to deeper layers. In particular, the relaxation of Ga3 seems significant, although our CTR analysis finds an almost negligible displacement from its bulk position. Overall, it can be concluded that there is good agreement with the DFT calculations, given that relatively small differences between the two methods can be understood by considering experimental uncertainties of the order of 0.01–0.02 Å and possible systematic differences, such as different lattice parameters, between the models used in the DFT study and the present experiment. Although the CTRs are not particularly sensitive to the oxygen positions, there is also an overall good agreement between theory and experiment, in particular with respect to the oxygen atoms surrounding the topmost  $\text{Ga}_{2\text{tet}}$  and  $\text{Ga}_{1\text{oct}}$  showing the largest displacements in the range of 0.05–0.1 Å. Table S4 shows in detail the atomic distances between Ga and O atoms in the topmost layer, as found by Bermudez<sup>19</sup> and our study, and shows a maximum deviation of about 0.05 Å. The uncovered (100)B termination is also in agreement with previous experimental studies, either on cleaved bulk crystals<sup>14</sup> or on an ultrathin  $\text{Ga}_2\text{O}_3$  layer, grown by selective oxidation of a  $\text{CoGa}(001)$  single crystal.<sup>37,38</sup> The results of a recent photo-electron diffraction study<sup>16</sup> are not in good agreement with our study and the previously mentioned DFT studies. Although that study also favors the (100)B termination, the atomic positions found disagree. For example, Kilian *et al.* find that the distance along the surface normal direction between the  $\text{Ga}_{1\text{oct}}$  and  $\text{Ga}_{2\text{tet}}$  atoms is 1.17 Å, thereby enlarging the bulk value by 41%. This is not at all in accord with the nearly bulk-terminated structure found in this study, where the typical displacements from the bulk are in the order of 1%.

In summary, we have comprehensively characterized the as-cleaved  $\beta$ - $\text{Ga}_2\text{O}_3(100)$  by combining AFM, LEED, and SXRD. The surface morphology indicates that the cleaved surface is single-terminated, most likely with terrace sizes exceeding the typical AFM scan area in the order of several square micrometers. LEED and in-plane reciprocal space mapping by SXRD reveal a well-ordered unreconstructed surface. Surface crystallography by CTR measurement and fitting enables us to obtain a high-resolution structure, consisting of

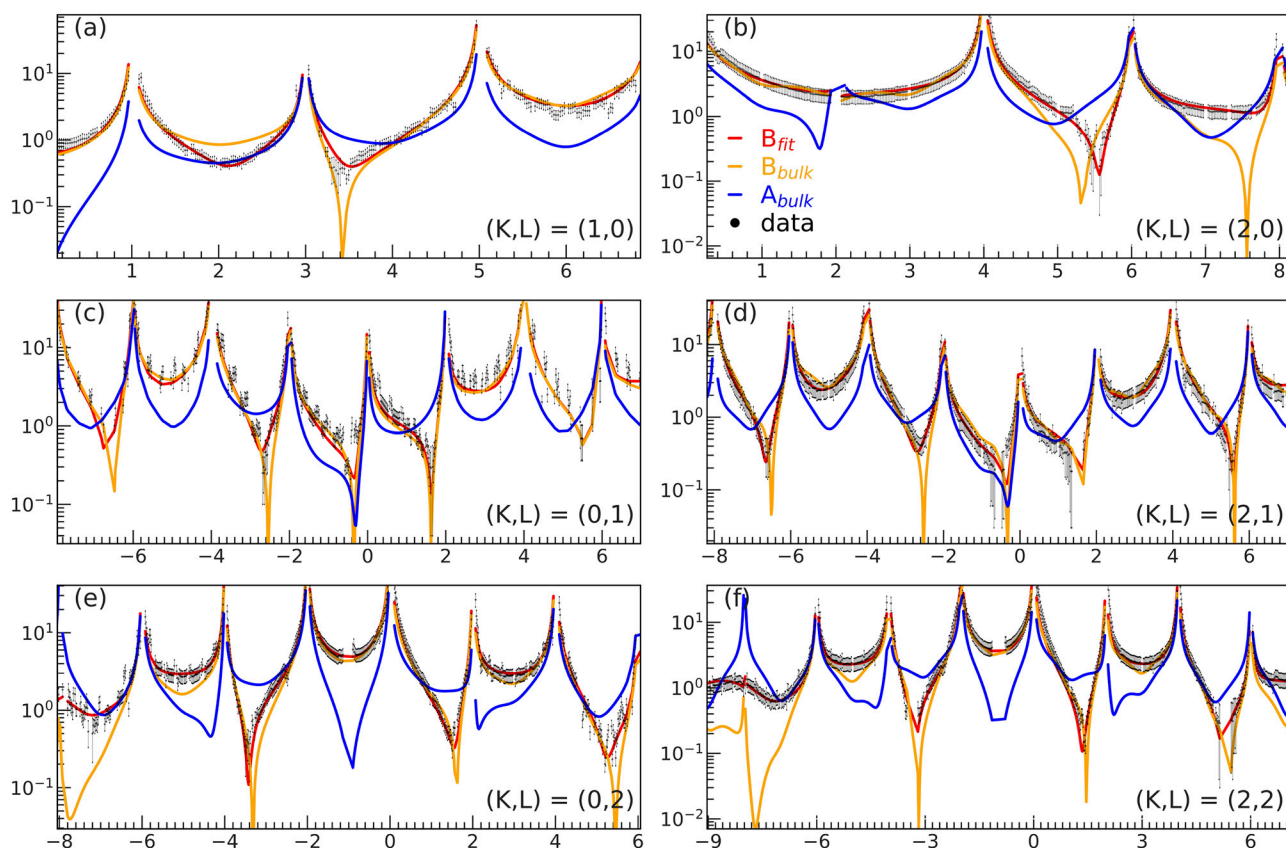


**FIG. 4.** Comparison of experimental, simulated, and fitted CTR data. The bulk structure factors ( $F$ ) are shown as black circles with error bars. Simulated CTRs for terminations A and B are represented by blue and yellow lines. Fitted CTRs for termination B are indicated by a red line. Each CTR is indexed by  $(K, L)$  and plotted as a function of  $H$ .

the so-called (100)B termination with relatively small (maximum  $0.1 \text{ \AA}$ ) atomic relaxations from bulk positions. This structure is in excellent agreement with a DFT study and is in line with other experimental studies on similar surfaces. Such a nearly bulk-terminated surface, formed along a cleave plane, is also the most obvious when considering that the longest (and weakest) Ga–O bonds are broken and that it constitutes a non-polar surface. The high-resolution crystallographic surface structure determined in this study is important for the fracture properties of  $\beta\text{-Ga}_2\text{O}_3$ , thin film growth on  $\beta\text{-Ga}_2\text{O}_3(100)$  substrates and electronic surface properties of such substrates or exfoliated flakes. In addition, the accurate determination of the single crystal surface structure, as presented in this study, is essential for future investigations on gas adsorption, particularly when  $\beta\text{-Ga}_2\text{O}_3$  is employed in gas-sensing applications. A comprehensive understanding of adsorption mechanisms requires precise knowledge of the surface structure. These insights are expected to play a significant role in the development of advanced sensors based on our observations.

See the [supplementary material](#) for the bulk and fitted fractional atomic positions, as well as the analysis of the experimental data.

This project is funded by the Deutsche Forschungsgemeinschaft (DFG, German Research Foundation) under Project No. 491040331.

We acknowledge SOLEIL for the provision of synchrotron radiation facilities, and we would like to thank the beamline staff for assistance in using beamline SIXS under proposal 20230826. We also acknowledge DESY (Hamburg, Germany), a member of the Helmholtz Association HGF, for the provision of experimental facilities. Parts of this research were carried out at DESY NanoLab.

## AUTHOR DECLARATIONS

### Conflict of Interest

The authors have no conflicts to disclose.

### Author Contributions

**Ming-Chao Kao:** Conceptualization (equal); Data curation (equal); Formal analysis (equal); Investigation (equal); Methodology (equal); Software (equal); Writing – original draft (equal). **Lukas Paul Schewe:** Investigation (supporting); Writing – review & editing (supporting). **Arub Akhtar:** Investigation (supporting); Writing – review & editing (supporting). **Alina Vlad:** Investigation (supporting); Writing – review & editing (supporting). **Thomas F. Keller:** Methodology (supporting); Writing – review & editing (supporting). **Karsten Henkel:** Writing – review & editing (supporting). **Saud Bin Anooz:** Writing – review & editing (supporting). **Andreas Popp:** Funding acquisition (lead);

Supervision (supporting); Writing – review & editing (supporting). **Zbigniew Galazka**: Funding acquisition (lead); Methodology (lead); Resources (lead); Writing – review & editing (supporting). **Jan Ingo Flege**: Funding acquisition (lead); Supervision (lead); Writing – review & editing (supporting). **Andreas Stierle**: Funding acquisition (lead); Supervision (lead); Writing – review & editing (equal). **Vedran Vonk**: Conceptualization (equal); Formal analysis (equal); Funding acquisition (lead); Investigation (equal); Methodology (lead); Software (equal); Supervision (lead); Writing – original draft (equal); Writing – review & editing (equal).

## DATA AVAILABILITY

The data that support the findings of this study are available from the corresponding author upon reasonable request.

## REFERENCES

- H. H. Tippins, "Optical absorption and photoconductivity in the band edge of  $\beta$ -Ga<sub>2</sub>O<sub>3</sub>," *Phys. Rev.* **140**, A316 (1965).
- Z. Galazka, " $\beta$ -Ga<sub>2</sub>O<sub>3</sub> for wide-bandgap electronics and optoelectronics," *Semicond. Sci. Technol.* **33**, 113001 (2018).
- M. Higashiwaki, K. Sasaki, A. Kuramata, T. Masui, and S. Yamakoshi, "Gallium oxide (Ga<sub>2</sub>O<sub>3</sub>) metal-semiconductor field-effect transistors on single-crystal  $\beta$ -Ga<sub>2</sub>O<sub>3</sub> (010) substrates," *Appl. Phys. Lett.* **100**, 013504 (2012).
- M. Higashiwaki, K. Sasaki, H. Murakami, Y. Kumagai, A. Koukitu, A. Kuramata, T. Masui, and S. Yamakoshi, "Recent progress in Ga<sub>2</sub>O<sub>3</sub> power devices," *Semicond. Sci. Technol.* **31**, 034001 (2016).
- M. Higashiwaki, K. Sasaki, T. Kamimura, M. Hoi Wong, D. Krishnamurthy, A. Kuramata, T. Masui, and S. Yamakoshi, "Depletion-mode Ga<sub>2</sub>O<sub>3</sub> metal-oxide-semiconductor field-effect transistors on  $\beta$ -Ga<sub>2</sub>O<sub>3</sub> (010) substrates and temperature dependence of their device characteristics," *Appl. Phys. Lett.* **103**, 123511 (2013).
- M. Higashiwaki, K. Sasaki, A. Kuramata, T. Masui, and S. Yamakoshi, "Development of gallium oxide power devices," *Phys. Status Solidi A* **211**, 21–26 (2014).
- M. J. Tadjer, "Toward gallium oxide power electronics," *Science* **378**, 724–725 (2022).
- X. Wang, Z. Chen, D. Guo, X. Zhang, Z. Wu, P. Li, and W. Tang, "Optimizing the performance of a  $\beta$ -Ga<sub>2</sub>O<sub>3</sub> solar-blind uv photodetector by compromising between photoabsorption and electric field distribution," *Opt. Mater. Express* **8**, 2918–2927 (2018).
- J. Kim, S. Oh, M. A. Mastro, and J. Kim, "Exfoliated  $\beta$ -Ga<sub>2</sub>O<sub>3</sub> nano-belt field-effect transistors for air-stable high power and high temperature electronics," *Phys. Chem. Chem. Phys.* **18**, 15760–15764 (2016).
- X. Wang, D. Liu, X. Wang, Z. Liu, and S. Luo, "Tuning the optoelectronic properties of two-dimensional  $\beta$ -Ga<sub>2</sub>O<sub>3</sub> using surface passivation and the layer thickness," *Comput. Mater. Sci.* **246**, 113346 (2025).
- S. Pearton, J. Yang, P. H. Cary, F. Ren, J. Kim, M. J. Tadjer, and M. A. Mastro, "A review of Ga<sub>2</sub>O<sub>3</sub> materials, processing, and devices," *Appl. Phys. Rev.* **5**, 011301 (2018).
- M. R. Delgado and C. O. Areán, "Surface chemistry and pore structure of  $\beta$ -Ga<sub>2</sub>O<sub>3</sub>," *Mater. Lett.* **57**, 2292–2297 (2003).
- H. Zhai, Z. Wu, and Z. Fang, "Recent progress of Ga<sub>2</sub>O<sub>3</sub>-based gas sensors," *Ceram. Int.* **48**, 24213–24233 (2022).
- M. Busch, E. Meyer, K. Irmscher, Z. Galazka, K. Gärtner, and H. Winter, "Fast atom diffraction from a  $\beta$ -Ga<sub>2</sub>O<sub>3</sub> (100) surface," *Appl. Phys. Lett.* **105**, 051602 (2014).
- T. Lovejoy, E. Yitamben, N. Shamir, J. Morales, E. Villora, K. Shimamura, S. Zheng, F. Ohuchi, and M. Olmstead, "Surface morphology and electronic structure of bulk single crystal  $\beta$ -Ga<sub>2</sub>O<sub>3</sub>," *Appl. Phys. Lett.* **94**(100), 081906 (2009).
- A. S. Kilian, A. de Siervo, R. Landers, G. J. P. Abreu, M. S. Castro, T. Back, and A. Pancotti, "Unravelling the surface structure of  $\beta$ -Ga<sub>2</sub>O<sub>3</sub>," *RSC Adv.* **13**(100), 28042–28050 (2023).
- S. Mu, M. Wang, H. Peelaers, and C. G. Van de Walle, "First-principles surface energies for monoclinic Ga<sub>2</sub>O<sub>3</sub> and Al<sub>2</sub>O<sub>3</sub> and consequences for cracking of  $\beta$ -(Al<sub>x</sub>Ga<sub>1-x</sub>)<sub>2</sub>O<sub>3</sub>," *APL Mater.* **8**, 081110 (2020).
- Y. Hinuma, T. Gake, and F. Oba, "Band alignment at surfaces and heterointerfaces of Al<sub>2</sub>O<sub>3</sub>, Ga<sub>2</sub>O<sub>3</sub>, In<sub>2</sub>O<sub>3</sub>, and related group-III oxide polymorphs: A first-principles study," *Phys. Rev. Mater.* **3**, 084605 (2019).
- V. Bermudez, "The structure of low-index surfaces of  $\beta$ -Ga<sub>2</sub>O<sub>3</sub>," *Chem. Phys.* **323**, 193–203 (2006).
- Z. Galazka, "Growth of bulk  $\beta$ -Ga<sub>2</sub>O<sub>3</sub> single crystals by the Czochralski method," *J. Appl. Phys.* **131**, 125105 (2022).
- Z. Galazka, A. Fiedler, A. Popp, S. Ganschow, A. Kwasniewski, P. Seyidov, M. Pietsch, A. Dittmar, S. B. Anooz, K. Irmscher *et al.*, "Bulk single crystals and physical properties of  $\beta$ -(Al<sub>x</sub>Ga<sub>1-x</sub>)<sub>2</sub>O<sub>3</sub> (x = 0–0.35) grown by the czochralski method," *J. Appl. Phys.* **133**, 075105 (2023).
- S. Geller, "Crystal structure of  $\beta$ -Ga<sub>2</sub>O<sub>3</sub>," *J. Chem. Phys.* **33**, 676–684 (1960).
- J. Åhman, G. Svensson, and J. Albertsson, "A reinvestigation of  $\beta$ -gallium oxide," *Acta Crystallogr., Sect. C* **52**, 1336–1338 (1996).
- Y. Ota, "Band alignment of  $\beta$ -(Al<sub>x</sub>Ga<sub>1-x</sub>)<sub>2</sub>O<sub>3</sub> alloys via atomic solid-state energy scale approach," *AIP Adv.* **10**, 115123 (2020).
- A. Stierle, T. F. Keller, H. Noei, V. Vonk, and R. Roehlsberger, "DESY NanoLab," *J. Large-Scale Res. Facil.* **2**, A76 (2016).
- D. Nečas and P. Klapetek, "Gwyddion: An open-source software for SPM data analysis," *Open Phys.* **10**, 181–188 (2012).
- A. Dawiec, Y. Garreau, J. Bisou, S. Hustache, B. Kanoute, F. Picca, G. Renaud, and A. Coati, "Real-time control of the beam attenuation with XPAD hybrid pixel detector," *J. Instrum.* **11**, P12018 (2016).
- S. Roobol, W. Onderwaater, J. Drnec, R. Felici, and J. Frenken, "*BINoculars*: Data reduction and analysis software for two-dimensional detectors in surface x-ray diffraction," *J. Appl. Crystallogr.* **48**, 1324–1329 (2015).
- E. Vlieg, see [https://www.esrf.fr/computing/scientific/joint\\_projects/ANA-ROD/index.html](https://www.esrf.fr/computing/scientific/joint_projects/ANA-ROD/index.html) for "A Concise Rod Manual" (2001).
- I. Robinson and D. Tweet, "Surface x-ray diffraction," *Rep. Prog. Phys.* **55**, 599 (1992).
- I. K. Robinson, "Crystal truncation rods and surface roughness," *Phys. Rev. B* **33**, 3830 (1986).
- G. Wagner, M. Baldini, D. Gogova, M. Schmidbauer, R. Schewski, M. Albrecht, Z. Galazka, D. Klimm, and R. Fornari, "Homoepitaxial growth of  $\beta$ -Ga<sub>2</sub>O<sub>3</sub> layers by metal-organic vapor phase epitaxy," *Phys. Status Solidi A* **211**, 27–33 (2014).
- W. de Poel, S. Pinteau, J. Drnec, F. Carla, R. Felici, P. Mulder, J. A. Elemans, W. J. van Enckevort, A. E. Rowan, and E. Vlieg, "Muscovite mica: Flatter than a pancake," *Surf. Sci.* **619**, 19–24 (2014).
- R. Schewski, M. Baldini, K. Irmscher, A. Fiedler, T. Markurt, B. Neuschulz, T. Remmele, T. Schulz, G. Wagner, Z. Galazka *et al.*, "Evolution of planar defects during homoepitaxial growth of  $\beta$ -Ga<sub>2</sub>O<sub>3</sub> layers on (100) substrates—A quantitative model," *J. Appl. Phys.* **120**, 225305 (2016).
- P. Tasker, "Stability of ionic-crystal surfaces," *J. Phys. C* **12**, 4977–4984 (1979).
- J. Goniakowski, F. Finocchi, and C. Noguera, "Polarity of oxide surfaces and nanostructures," *Rep. Prog. Phys.* **71**, 016501 (2008).
- A. Vlad, A. Stierle, M. Marsman, G. Kresse, I. Costina, H. Dosch, M. Schmid, and P. Varga, "Metastable surface oxide on CoGa(100): Structure and stability," *Phys. Rev. B* **81**, 115402 (2010).
- A. Stierle, R. Streitl, P. Nolte, A. Vlad, I. Costina, M. Marsman, G. Kresse, E. Lundgren, J. N. Andersen, R. Franchy *et al.*, "Real time observation of ultrathin epitaxial oxide growth during alloy oxidation," *New J. Phys.* **9**, 331 (2007).